Increased Brain Glucose Utilization in Salla Disease (Free Sialic Acid Storage Disorder)

Hanna Suhonen-Polvi, Tarja Varho, Liisa Metsähonkala, Leena Haataja, Ulla Ruotsalainen, Merja Haaparanta, Jörgen Bergman, Olof Solin, Tuula Äärimaa, Irma Holopainen, Leena Vainionpää, Tuula Manner, Satu Jääskeläinen, Martin Renlund, Matti Sillanpää and Pertti Aula

Departments of Pediatric Neurology, Medical Genetics, Anesthesiology and Clinical Neurophysiology, University of Turku, Turku; Turku PET Center, Turku; Department of Pediatrics, University of Oulu, Oulu; and Department of Obstetrics and Gynecology, University of Helsinki, Helsinki, Finland

Salla disease is an autosomal recessive lysosomal free sialic acid storage disorder characterized by psychomotor retardation and ataxia. MRI studies have revealed evidence of dysmyelination, but the biological mechanism of the brain dysfunction is unknown. **Methods:** Nine patients with Salla disease (age 2.5 mo–42 y) presenting the disease in varying degrees of severity were studied by PET using 2-fluoro-2-deoxy-D-glucose (FDG) as a tracer. Local cerebral metabolic rates for glucose (LCMRGlc) in individual brain regions were compared with controls. **Results:** The FDG PET results showed significantly increased LCMRGlc values in the frontal and sensorimotor cortex and especially in the basal ganglia of the patients. Cerebellar hypometabolism was present in all seven patients with marked ataxia, whereas the less severely affected patients without obvious ataxia had normal or even high glucose uptake in the cerebellum. **Conclusion:** The increased cerebral glucose utilization is a constant finding in Salla disease and may reflect the basic defect of the sialic acid metabolism in this disorder. The FDG PET findings in the cerebellum suggest a correlation between glucose uptake and the severity of the clinical symptoms.

Key Words: Salla disease; PET; fluorodeoxyglucose; cerebral metabolism

J Nucl Med 1999; 40:12–18

Salla disease is a recessively inherited lysosomal storage disorder characterized by free sialic acid (*N*-acetylneuraminic acid [NANA]) storage in the lysosomes of various tissues and its hyperexcretion in urine (*1,2*). Sialic acid accumulation is caused by defective transport of NANA across the lysosomal membrane to the cytoplasm due to the impaired function of a specific proton-driven transport mechanism (*3*). The gene locus of Salla disease has been assigned to a restricted region on the long arm of chromosome 6 (6q14–6q15) using genetic linkage analysis (*4,5*). The physical map of the critical deoxyribonucleic acid (DNA) region has recently been constructed (*6*), providing a good basis for future isolation of the gene coding for the putative transport protein.

Received Dec. 31, 1997; revision accepted Apr. 30, 1998.

For correspondence or reprints contact: Tarja Varho, MD, Department of Medical Genetics, University of Turku, FIN-20520, Turku, Finland.

More than 90 patients with Salla disease are known in Finland, where the disorder is unusually frequent, but sporadic cases have been reported in other populations as well (*7–9*). The main feature of Salla disease is severe psychomotor retardation. The first symptoms are usually present at 3–6 mo of age as muscular hypotonia, ataxia, transient nystagmus and retarded motor development. Developmental delay progresses slowly, and more pronounced deterioration becomes evident during the second or third decade of life. Life expectancy is only slightly decreased. There is marked variation in phenotypic severity between patients. Most patients (approximately 85%) have a "conventional" course of the disease: they are able to walk and speak short sentences, whereas patients with the severe phenotype never learn to speak or become ambulant because of early-onset progressive spasticity and severe ataxia (*2*).

A neuropathological study of two patients with Salla disease showed markedly reduced cerebral white matter and corpus callosum hypoplasia (*10*). Histological examinations showed loss of axons and myelin sheaths accompanied by pronounced astrocytic proliferation in the cerebrum. Moderate loss of Purkinje cells was found in the cerebellum. A recent MRI study showed defective myelination and a hypoplastic corpus callosum in both the conventional and the severe forms of the disease (*11*). Global cerebral atrophy was seen earlier in the severely disabled patients.

PET is a functional imaging technique that allows in vivo noninvasive measurement of the concentration of radiopharmaceuticals labeled with positron emitters (*12*). [^{18}F]2-fluoro-2-deoxy-D-glucose (FDG) is the most frequently used tracer for the assessment of glucose metabolism in the central nervous system (*12*). It is transported into the cells and phosphorylated but not metabolized further. Local cerebral metabolic rates for glucose (LCMRGlc) are age dependent, increasing during childhood to values nearly twice as high as those reported for adult subjects and declining toward the end of the first decade to reach near-adult values by late adolescence (*13,14*).

To get more insight into the biological mechanism by which the accumulation of free sialic acid—an acidic monosaccharide—leads to brain dysfunction and dysmyelin-

ation, we wanted to measure the energy metabolism by FDG PET. Contrary to our expectations, the main finding in our patients with Salla disease was increased glucose metabolism in specific brain regions.

METHODS

Patients

Nine patients with Salla disease were studied (aged 2.5 mo to 42 y; mean, 17.2 y). Diagnosis had earlier been confirmed by measurement of free sialic acid excretion in urine, enlarged lysosomes in skin biopsy and DNA linkage analysis. There were six male and three female patients. All the patients were normal as newborns and did not have any neonatal problems, except for patient 3, who had nystagmus soon after birth. Their growth was normal (height −2.2 SD to +1.2 SD), with the exception of one severely disabled patient (patient 6), whose height was −6.2 SD. The six patients with conventional course of the disease (patients 2, 3, 4, 5, 7 and 9) had mild to moderate ataxia and psychomotor retardation with IQs ranging from 20 to 60. The 2.5-mo-old girl (patient 1) was a sibling to patient 3, and her diagnosis was made during the neonatal period in accordance with her parents' wishes. At 2.5 mo, she had poor eye contact but was otherwise neurologically normal. Two patients (patients 6 and 8) were severely affected with marked spasticity, epilepsy and profound mental retardation (IQ < 20). Patient 6 had had epilepsy from the age of 2 y, but had been free from epileptic seizures and off medication for the past 2 y. Patient 8 had had epilepsy from 4 y old and was still on antiepileptic medication (valproic acid). The other patients did not have any regular medication. None of the patients was on a special diet. The clinical details of the patients are presented in Table 1.

The study was approved by the Joint Ethics Committee of the Turku University and the Turku University Central Hospital, and informed consent was obtained from all legal guardians.

PET

Preparation of FDG. The FDG was synthesized using the method of Hamacher et al. (*15*). The specific activity at the end of the synthesis was approximately 2 Ci/μmol, and the radiochemical purity exceeded 98% (*16*).

Image Acquisition. The studies were performed using an eight-ring ECAT 931/08-tomograph (Siemens/CTI Inc., Knoxville, TN) with the imaging planes oriented parallel to the canthomeatal line. The axial resolution was 6.7 mm, and the in-plane resolution was 6.5 mm (full width of the half maximum). Tissue attenuation was measured with the transmission scan using a removable ring source containing ^{68}Ge/Ga.

General anesthesia was used to achieve the desired quiet state during scanning. All patients fasted 4 h before PET scan. On arrival, glycopyrrolate 4 μg/kg was administered. Anesthesia was induced with thiopentone 3–5 mg/kg intravenously and fentanyl 2–3 μg/kg intravenously. Vecuronium 100–120 μg/kg was administered intravenously to facilitate endotracheal intubation. The patients were mechanically ventilated with oxygen in nitrous oxide (30/70%) to maintain the end-tidal CO_2 between 4.0 and 5.0 kPa. Blood pressure, heart rate and peripheral oxygen saturation were monitored noninvasively. On completion of the investigation, the neuromuscular blockage was reversed with neostigmine 50 μg/kg and glycopyrrolate 10 μg/kg intravenously.

A rapid injection of 0.1 mCi/kg FDG was administered intravenously. Simultaneously, a dynamic scan of the brain was started and continued for 55 min (4 × 30 s, 3 × 60 s, 10 × 300 s). An "arterialized" blood sample for the measurement of plasma radioactivity was taken once during each time frame. The radioactivity concentration was measured with an automated gamma counter (Wizard 3" 1480, Wallac Inc., Turku, Finland) and calibrated to the PET scanner. The examination of the youngest patient (patient 1) was performed according to Suhonen-Polvi et al. (*17*), including two phases: (a) a heart study (beginning of the blood curve), and (b) a brain study. Plasma glucose concentrations were measured three times during the PET examination. All patients were normoglycemic and the measured plasma glucose was 5.0 ± 0.48 mmol/L. Continuous electroencephalogram (EEG) recordings were performed with an 8-channel cassette EEG recorder (Oxford Medilog 9000-II; Oxford Medical Ltd., Abingdon Oxon, England) on 7 patients (patients 1, 2, 3, 4, 6, 8 and 9) during PET studies.

Image Processing. Region of interest (ROI) analysis was performed on Hann-filtered, 256 × 256 PET reconstructions (cutoff frequency 0.5), which were corrected for deadtime and decay and the measured photon attenuation. Elliptical or circular ROIs were placed on each plane, visualizing the cortical gray matter structures: the frontal, sensorimotor (precentral and postcentral gyri), temporal, parietal, and occipital cortex and the subcortical structures (basal ganglia, thalamus, and cerebellum). The mean LCMRGlc of each anatomic region was calculated.

TABLE 1
Clinical and MRI Data of the Salla Disease Patients

Patient no.	Age at PET scan	First symptoms/age	Walking	Speech	Ataxia	Spasticity	MRI
1	2.5 mo	Poor eye contact/2 mo	—	—	No	No	Normal
2	15 mo	Poor head control/5 mo	No	Words	++	No	Defective myelination, CCH
3	35 mo	Nystagmus/<1 mo	No	One word	+++	No	Defective myelination, CCH
4	4 y	Muscular hypertonia/1 mo	No	Words	+++	No	Defective myelination, CCH
5	5 y	Ataxia/14 mo	Yes	Sentences	++	No	Defective myelination, CCH
6	12 y	Restless, enlarged liver/2 mo	No	No	+++	++	Defective myelination, CCH, brain atrophy
7	15 y	Muscular hypotonia/<1 y	Yes	Sentences	+	+	Defective myelination, CCH
8	17 y	Restless, tremor/2 mo	No	Two words	++	+++	Defective myelination, CCH, brain atrophy
9	42 y	Not known	No	One word	++	+++	Defective myelination, CCH, brain atrophy

+ = mild ataxia/spasticity; ++ = moderate ataxia/spasticity; +++ = severe ataxia/spasticity; CCH = corpus callosum hypoplasia.

Calculation of Regional Glucose Utilization. The differential equations governing the three-compartment FDG tracer-kinetic model have been described previously (*18*). The plasma and tissue time-activity curves were analyzed graphically (*19*) to quantitate the fractional rate of tracer phosphorylation, K_i. The rate of glucose utilization is obtained by multiplying K_i by the plasma glucose concentration $[Glc]_p$, and dividing by a lumped constant term (LC), i.e., the rate of glucose utilization = $([Glc]_p/LC) \times K_i$. The lumped constant accounts for differences in the transport and phosphorylation of FDG and glucose (*20*). The LC used in this study was 0.52 (*21*).

Control Materials. In FDG PET studies, the age dependency of the cerebral glucose metabolism has to be considered. Because healthy children were considered unacceptable as controls for ethical reasons, control data for different age groups had to be taken from the following sources:

1. <1 y: 12 infants with suspected hypoxic-ischemic brain injury, but with subsequent normal development (*14*)
2. 1–2 y and 3–8 y: 16 children with transient neurological disorders from material from Chugani et al. (*13*)
3. 9–20 y: nine 9–17-y-old children with migraine without daily medication during the study (unpublished data)
4. >20 y: seven voluntary 24–25-y-old healthy male medical students (unpublished data)

Control groups 1, 3 and 4 were studied with the same imaging protocol as the patients. Although control group 2 was studied in a different institution, the protocol used was in principle the same. None of the controls were examined under anesthesia or sedation.

MRI

Brain MRI was performed using 1.0- or 1.5-T MR imagers on all nine Salla patients before the FDG PET studies.

Statistical Analyses

The glucose metabolic rates of the different brain areas of each patient were compared with the corresponding values of the age-matched control group pairs using a paired *t* test. $P < 0.05$ was considered statistically significant. Age correlation was studied with Spearman's correlation coefficients.

RESULTS

PET

The Salla disease patients had significantly higher LCMRGlc than the controls in the frontal cortex ($P = 0.02$, Fig. 1A), the sensorimotor cortex ($P = 0.04$, Fig. 1B) and the basal ganglia ($P = 0.007$, Fig. 1C). The LCMRGlc of the other brain regions (parietal, temporal and occipital cortex, thalamus and cerebellum) did not differ significantly from the controls. Compared with the controls, the severely affected patients (6 and 8) also had significantly higher LCMRGlc in the temporal cortex ($P = 0.004$), but considerably lower LCMRGlc in the cerebellum ($P = 0.03$). All seven patients with marked ataxia showed decreased glucose utilization in the cerebellum ($P = 0.002$), whereas the LCMRGlc values of the patients without obvious ataxia (patients 1 and 7) were within normal range or even high in the cerebellum (Fig. 1D). The LCMRGic values did not correlate significantly with age for any brain region analyzed ($r = 0.04$–0.54, $P > 0.05$). The detailed LCMRGlc data are given in Table 2.

None of the patients showed epileptogenic activity in the EEG recording during the FDG PET study.

MRI

All patients except patient 1 gave findings of defective myelination: an abnormal high signal intensity of subcortical white matter in the cerebrum on T2-weighted axial images. They also had a clearly hypoplastic corpus callosum. The severely affected patients (patients 6 and 8) and the 42-y-old patient with marked deterioration (patient 9) had atrophic changes cortically and centrally in the cerebrum and particularly in the cerebellum. The 15-y-old girl (patient 7) with only minor signs of ataxia had no atrophy in the cerebellum. The 2.5-mo-old girl (patient 1) whose neurological findings were within the normal limits was the only one without any abnormalities on MRI. All the patients had normal MRI in the basal ganglia.

The FDG PET and MRI findings of patient 8 are shown in Figure 2.

DISCUSSION

To our knowledge, this is the first FDG PET study in Salla disease, a lysosomal free sialic acid storage disorder leading to severe mental retardation and ataxia. Increased glucose utilization in the basal ganglia, sensorimotor cortex and frontal cortex was detected. Glucose hypermetabolism is an unusual finding in disorders of the central nervous system. In contrast, local or global reduction of glucose utilization has been found in some other neurodegenerative diseases. Batten's disease (late infantile and juvenile neuronal ceroid lipofuscinosis) is the only other childhood-onset lysosomal storage disorder studied so far by FDG PET (*22,23*). The main symptoms in juvenile Batten's disease are progressive visual impairment, dystonia, dysarthria, myoclonus and later on variable degrees of mental retardation. Decreased glucose metabolism starting in the calcarine area and spreading to the entire cortex with normal uptake only in the basal ganglia and brainstem was found. In late infantile Batten's disease, FDG PET studies showed severe generalized hypometabolism associated with progressive cerebral atrophy on anatomical neuroimaging. In Huntington's disease, the decline in glucose utilization has been localized especially to the caudate nucleus without significant global hypometabolism (*24*).

Hypermetabolism in the cortical areas, basal ganglia and also in the cerebellum has been found in patients with Friedreich's ataxia (FA), a chronic progressive neurological disorder inherited as an autosomal recessive trait (*25*). Ambulatory FA patients had widespread increased glucose uptake, which decreased in a regionally specific manner along the progression of the disease with the exception of the basal ganglia. The decline was considered to be due to the

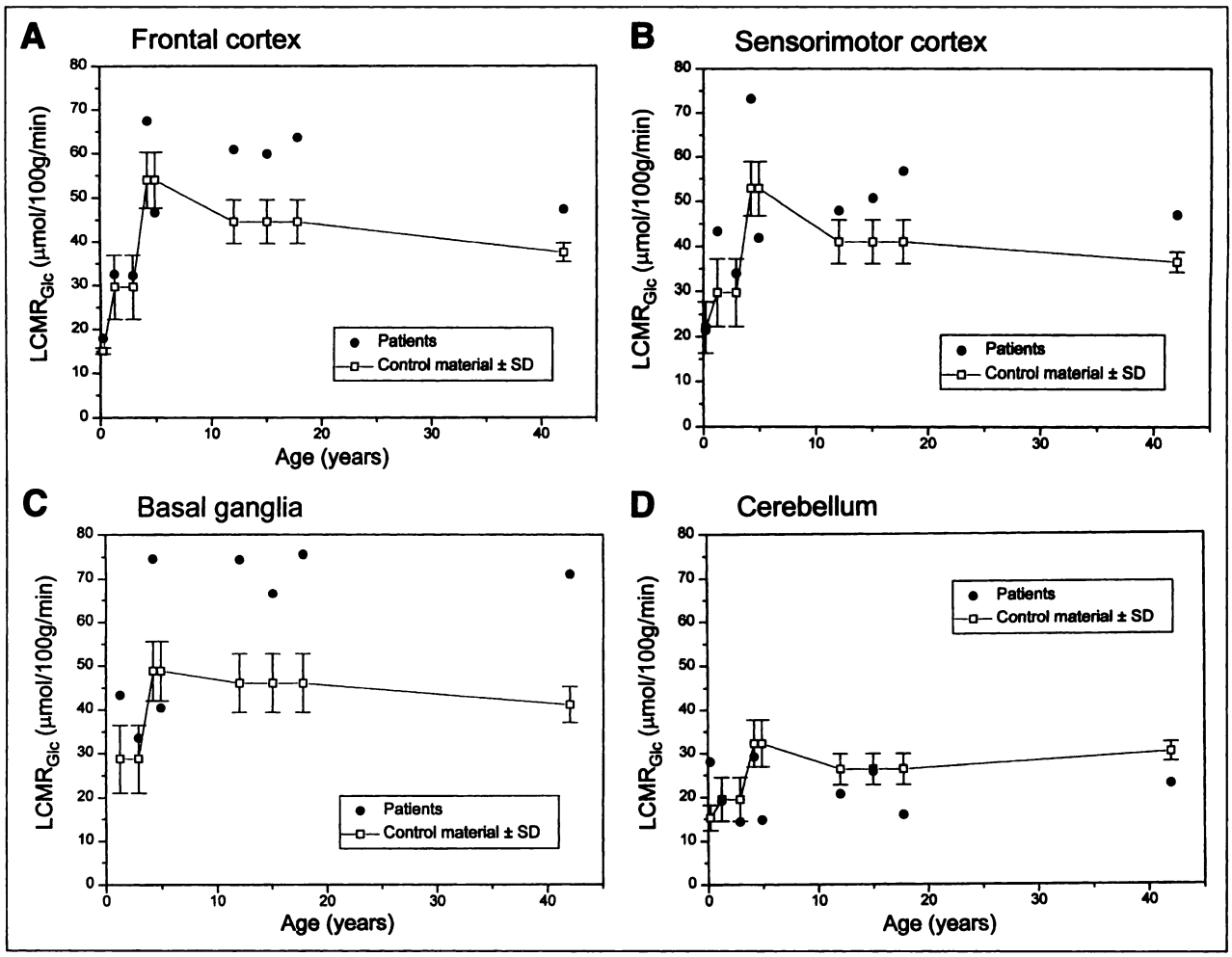

FIGURE 1. Mean local cerebral metabolic rates for glucose (µmol/100 g/min) of each patient with Salla disease and corresponding control values (±SD) using FDG in PET study: (A) frontal cortex; (B) sensorimotor cortex; (C) basal ganglia; (D) cerebellum.

loss of neuronal connections. The glucose hypermetabolism in FA may reflect an increased requirement for glycolysis due to the defective oxidation of pyruvate, the suggested mechanism for abnormal carbohydrate metabolism in FA (*26*). In addition to FA, only a few studies suggesting hypermetabolism in FDG PET have been reported (*27–29*).

The basic defect in Salla disease is in the transport of the major sialic acid, NANA, from the lysosomes to be reutilized or degraded in the cytoplasm (*3*). Thereby the turnover of sialic acid is blocked, and the reutilization of free NANA liberated in the lysosomes by neuraminidase is slowed down. Theoretically this may cause a shortage of NANA in the cytoplasm, leading to an excessive need for glucose, the precursor of NANA (Fig. 3). Sialic acid is a major component of the myelin, and its lysosomal accumulation may cause deprivation in myelin biosynthesis (*30*). It is also possible that the defective myelination, a constant finding in Salla disease, or lysosomal accumulation itself might lead to fundamental disruption of normal cell functions such as oxidative phosphorylation, thereby increasing energy demand and glucose uptake. The interplay between the free sialic acid storage in the lysosomes, dysmyelination and high glucose uptake in FDG PET needs further studies to understand the central nervous system pathogenesis of Salla disease.

Epileptogenic activity, a known cause of increased glucose utilization (*31*), was excluded in our study by continuous EEG recordings during FDG PET. Neither of the two patients with epilepsy had ictal EEG during PET. All but one (patient 1) of our patients needed general anesthesia for FDG PET because of poor cooperation, ataxia and involuntary movements. For ethical reasons the control persons were not studied under anesthesia. Data on the effects of anesthetics on glucose metabolism in FDG PET are not well documented. However, it seems unlikely that anesthesia would increase the glucose utilization, because anesthesia generally decreases cerebral blood flow and cerebral metabolism (*32*). Also, the few FDG PET studies on intravenously administered benzodiazepines and barbiturates have shown significant reduction in glucose metabolism (*33,34*). Furthermore, none of the controls were studied under anesthesia, which could have caused hypometabolism in the control groups.

The use of common lumped constant in normal controls

TABLE 2
Mean LCMRGlc Values (μmol/100 g/min) of Individual Brain Areas of Each Salla Disease Patient

Patient no.	Brain areas							
	Frontal (control ± SD)	Parietal	Sensorimotor	Temporal	Occipital	Basal ganglia	Thalamus	Cerebellum
1	17.9	20.5	21.5	16.7	19.3	—	42.3	28.1
	(15.1 ± 0.7)	(20.2 ± 1.9)	(22 ± 5.7)	(16.4 ± 1.7)	(15.8 ± 0.5)		(20 ± 0.3)	(15.3 ± 2.9)
2	32.5	30.2	43.4	30.9	30.3	43.4	36.0	19.2
	(29.7 ± 7.3)	(28.8 ± 7.1)	(29.7 ± 7.4)	(28.6 ± 8.5)	(30.4 ± 7.0)	(30.6 ± 7.7)	(29.5 ± 5.9)	(19.5 ± 5.0)
3	32.2	35.3	34.0	30.0	33.6	33.6	28.8	14.4
	(29.6 ± 7.3)	(28.8 ± 7.1)	(29.7 ± 7.4)	(28.6 ± 8.5)	(30.4 ± 7.0)	(30.6 ± 7.7)	(29.5 ± 5.9)	(19.5 ± 5.0)
4	67.5	74.2	73.2	64.7	59.0	74.6	67.6	29.2
	(54.0 ± 6.3)	(54.0 ± 5.8)	(52.9 ± 6.1)	(48.9 ± 5.9)	(56.4 ± 7.3)	(50.1 ± 6.8)	(49.5 ± 5.9)	(32.3 ± 5.4)
5	46.7	43.2	41.9	39.9	44.6	40.5	28.4	14.8
	(54.0 ± 6.3)	(54.0 ± 5.8)	(52.9 ± 6.1)	(48.9 ± 5.9)	(56.4 ± 7.3)	(50.1 ± 6.8)	(49.5 ± 5.9)	(32.3 ± 5.4)
6	60.1	60.9	48.0	48.4	38.9	74.4	79.0	20.7
	(44.6 ± 5.0)	(42.9 ± 4.7)	(41.0 ± 4.9)	(41.0 ± 5.4)	(38.1 ± 4.3)	(46.1 ± 6.7)	(42.3 ± 3.2)	(26.3 ± 3.5)
7	60.0	52.6	50.7	51.56	48.6	66.6	58.0	25.8
	(44.6 ± 5.0)	(42.9 ± 4.7)	(41.0 ± 4.9)	(41.0 ± 5.4)	(38.1 ± 4.3)	(46.1 ± 6.7)	(42.3 ± 3.2)	(26.3 ± 3.5)
8	63.7	46.0	56.8	47.8	43.1	75.6	59.1	16.0
	(44.6 ± 5.0)	(42.9 ± 4.7)	(41.0 ± 5.4)	(41.0 ± 5.4)	(38.1 ± 4.3)	(46.1 ± 6.7)	(42.3 ± 3.2)	(26.3 ± 3.5)
9	47.5	48.5	47	45.1	42.6	71.1	38.9	22.9
	(37.6 ± 2.3)	(37.1 ± 2.4)	(36.5 ± 2.2)	(36.6 ± 2.5)	(34.8 ± 2.4)	(41.2 ± 4.1)	(38.9 ± 4.2)	(30.2 ± 2.2)

LCMRGlc = local cerebral metabolic rates for glucose.

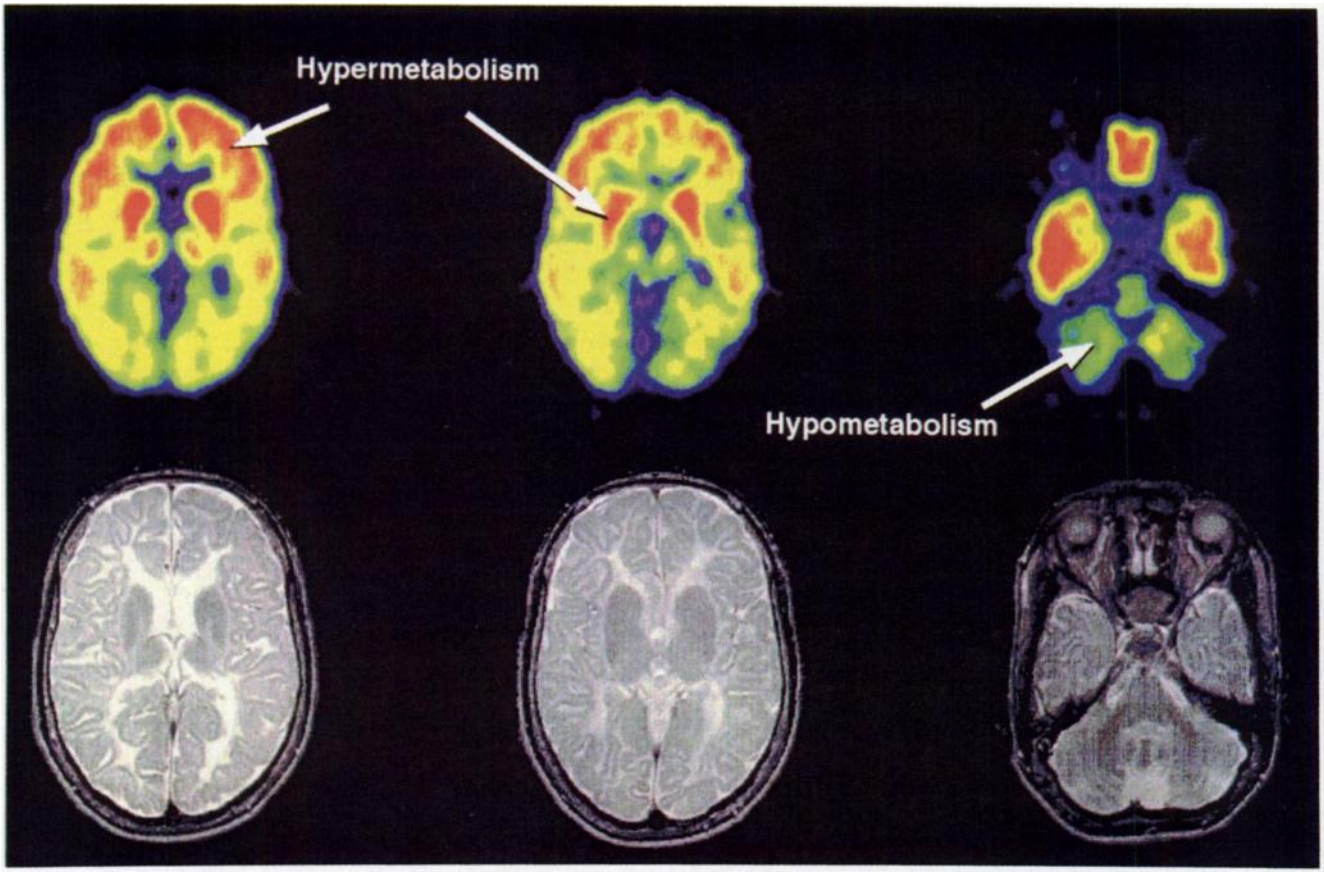

FIGURE 2. FDG PET (upper panel) of severely affected patient with Salla disease (patient 8) showing hypermetabolism in frontal cortex and basal ganglia and hypometabolism in cerebellum. Corresponding MRI slices are presented in lower panel.

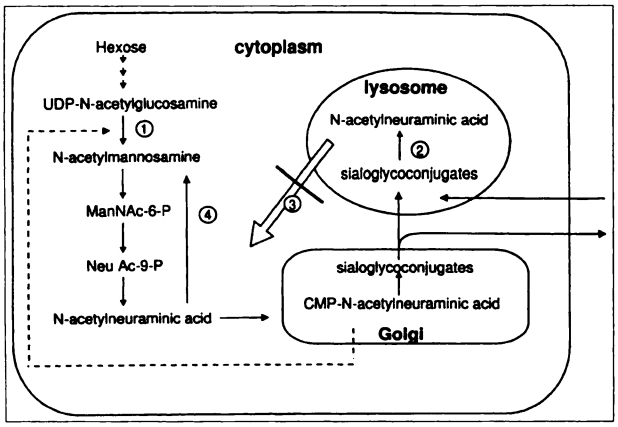

FIGURE 3. Main steps in sialic acid metabolism. Indicated enzymes and reactions: (1) UDP-*N*-acetylglucosamine-2-epimerase; (2) α-neuraminidase; (3) lysosomal membrane free sialic acid carrier; and (4) *N*-acetylneuraminate lyase.

and patients with a lysosomal storage disease may have some contribution to the metabolic rates for glucose and has to be taken into consideration, when interpreting the results. However, the patients had both increased and decreased regional values, so a systematical effect seems unlikely.

Cerebellar hypometabolism was present in all patients with ataxia. Cerebellar hypometabolism has earlier been found in patients with olivopontocerebellar atrophy (OPCA), a disease characterized by progressive cerebellar ataxia and athrophic changes in the cerebellum (*35*). The hypometabolism in OPCA correlated with cerebellar atrophy. The cerebellar hypometabolism in Salla disease correlated with the severity of clinical symptoms (ataxia) rather than with the structural changes found with MRI. Accordingly, the patient with the mildest symptoms (patient 7) had normal glucose utilization in the cerebellum and no atrophy on MRI. The hypermetabolism in her basal ganglia and frontal cortex was less significant than that of the others. These findings further suggest a possible correlation between glucose utilization and the severity of the clinical symptoms.

CONCLUSION

This FDG PET study showed that cerebral hypermetabolism, especially in the basal ganglia and frontal and sensorimotor cortex, is a constant feature of free sialic acid storage disorder, Salla disease. Hypometabolism, however, was seen in the cerebellum, and it correlated with the severity of clinical symptoms. The biological significance of these findings remains to be elucidated.

ACKNOWLEDGMENTS

This study was financially supported by the Rinnekoti Research Foundation, Espoo, Finland, and the Foundation for Pediatric Research, Finland. We thank the personnel of the Departments of Pediatrics and Child Neurology of the Turku University Central Hospital and Turku PET Center for pleasant cooperation. We are thankful to Pirkko Sonninen for MRI analyses and to Vesa Oikonen and Mika Klemetsö for advice with statistics and graphics.

REFERENCES

1. Aula P, Autio S, Raivio KO, et al. "Salla disease": a new lysosomal storage disorder. *Arch Neurol.* 1979;36:88–94.
2. Renlund M, Aula P, Raivio KO, et al. Salla disease: A new lysosomal storage disorder with disturbed sialic acid metabolism. *Neurology.* 1983;44:57–66.
3. Renlund M, Tietze F, Gahl WA. Defective sialic acid egress from isolated fibroblast lysosomes of patients with Salla disease. *Science.* 1986;232:759–762.
4. Haataja L, Schleutker J, Laine AP, et al. The genetic locus for free sialic acid storage disease maps to the long arm of chromosome 6. *Am J Hum Genet.* 1994;54:1042–1049.
5. Schleutker J, Laine AP, Haataja L, et al. Linkage disequilibrium utilized to establish a refined genetic position of the Salla disease locus on 6q14–q15. *Genomics.* 1995;27:286–292.
6. Leppänen P, Isosomppi J, Schleutker J, Aula P, Peltonen L. A physical map of the 6q14–q15 region harboring the locus for the lysosomal membrane sialic acid transport defect. *Genomics.* 1996;37:62–67.
7. Ylitalo V, Hagberg B, Rapola J, et al. Salla disease variants: sialoylaciduric encephalopathy with increased sialidase activity in two non-Finnish children. *Neuropediatrics.* 1986;17:44–47.
8. Sewell AC, Poets CF, Degen I, Stöss H, Pontz BF. The spectrum of free neuraminic acid storage disease in childhood: clinical, morphological and biochemical observations in three non-Finnish patients. *Am J Med Genet.* 1996;63:203–208.
9. Robinson RO, Fenson AH, Lake BD. Salla disease: rare or underdiagnosed? *Dev Med Child Neurol.* 1997;39:153–157.
10. Autio-Harmainen H, Oldfors A, Sourander P, Renlund M, Dammert K, Similä S. Neuropathology of Salla disease. *Acta Neuropathol.* 1988;75:481–490.
11. Haataja L, Parkkola R, Sonninen P, et al. Phenotypic variation and magnetic resonance imaging (MRI) in Salla disease, a free sialic acid storage disorder. *Neuropediatrics.* 1994;25:238–244.
12. Phelps ME, Mazziotta JC. Positron emission tomography: human brain function and biochemistry. *Science.* 1985;228:799–809.
13. Chugani HT, Phelps ME, Mazziotta JC. Positron emission tomography study on human brain functional development. *Ann Neurol.* 1987;22:487–497.
14. Kinnala A, Suhonen-Polvi H, Äärimaa T, et al. Cerebral metabolic rate for glucose during the six months of life: an FDG positron emission tomography study. *Arch Dis Child Fetal Neonatal Ed.* 1996;74:F153-F157.
15. Hamacher K, Coenen HH, Stöcklin G. Efficient stereospecific synthesis of no-carrier added 2-[^{18}F]-fluoro-2-deoxy-D-glucose using aminopolyether supported nucleophilic substitution. *J Nucl Med.* 1986;27:235–238.
16. Bergman J, Haaparanta M, Solin O. Computer controlled synthesis of 2-[^{18}]fluoro-2-deoxy-D-glucose (FDG). In: Sven-Johan Heselius, ed. *The Åbo Akademi Accelerator Laboratory Triennial Report 1990–1992.* Turku, Finland: University of Turku;1992:76–79.
17. Suhonen-Polvi H, Ruotsalainen U, Kinnala A, et al. FDG-PET in early infancy: simplified quantification methods to measure cerebral glucose utilization. *J Nucl Med.* 1995;36:1249–1254.
18. Sokoloff L, Reivich M, Kennedy C, et al. The [^{14}C]deoxyglucose method for the measurement of local cerebral glucose utilization: theory; procedure and normal values in the conscious and anesthetized albino rat. *J Neurochem.* 1977;28:897–916.
19. Patlak CS, Blasberg RG. Graphical evaluation of blood-to-brain transfer constants from multiple-time uptake data. Generalisations. *J Cereb Blood Flow Metab.* 1985;5:584–590.
20. Phelps ME, Huang S-C, Hoffman EJ, Selin C, Sokoloff L, Kuhl DE. Tomographic measurement of local cerebral glucose metabolic rate in humans with (F-18)2-fluoro-2-deoxy-D-glucose: validation of method. *Ann Neurol.* 1979;6:371–388.
21. Reivich M. Cerebral glucose consumption: methodology and validation. In: Reivich M, Alavi A, eds. *Positron Emission Tomography.* New York, NY: Alan R Liss; 1985:131–151.
22. Philippart M, Messa C, Chugani HT. Spielmeyer-Vogt (Batten, Spielmeyer-Sjögren) disease. Distinctive patterns of glucose utilization. *Brain.* 1994;117:1085–1092.
23. Philippart M, da Silva E, Chugani HT. The value of positron emission tomography in the diagnosis and monitoring of late infantile and juvenile lipopigment storage

disorders (so-called Batten or neuronal ceroid lipofuscinoses). *Neuropediatrics.* 1997;28:74–76.
24. Kuhl DE, Phelps ME, Markham CH, Metter EJ, Riege WH, Winter J. Cerebral metabolism and atrophy in Huntington's disease determined by 18-FDG and computed tomographic scan. *Ann Neurol.* 1982;12:425–434.
25. Gilman S, Junck L, Markel DS, Koeppe RA, Kluin KJ. Cerebral glucose hypermetabolism in Friedreich's ataxia detected with positron emission tomography. *Ann Neurol.* 1990;28:750–757.
26. Dijkstra U, Gabreëls F, Joosten E, et al. Freidreich's ataxia: intravenous pyruvate load to demonstrate a defect in pyruvate metabolism. *Neurology.* 1984;34:1493–1497.
27. Schwartz M, Duara R, Haxby J, et al. Down's syndrome in adults: brain metabolism. *Science.* 1983;221:781–783.
28. De Volder A, Bol A, Michel C, Cogneau M, Goffinet AM. Brain metabolism in children with the autistic syndrome: positron emission tomography analysis. *Brain Dev.* 1987;9:581–587.
29. Schapiro MB, Grady CL, Kumar A, et al. Regional cerebral glucose metabolism is normal in young adults with Down's syndrome. *J Cereb Blood Flow Metab.* 1990;10:199–206.
30. Chigorno V, Tettamanti G, Sonnino S. Metabolic processing of gangliosides by normal and Salla human fibroblasts in culture. *J Biol Chem.* 1996;271:21738–21744.
31. Engel J, Kuhl D, Phelps ME. Patterns of human local cerebral metabolism during epileptic seizures. *Science.* 1982;218:64–66.
32. Astrup J, Sørensen HR. Inhibition of cerebral oxygen and glucose consumption in the dog by hypothermia, pentobarbital and lidocaine. *Anesthesiology.* 1981;55:263–268.
33. Rockoff MA, Naughton KVH, Shapiro HM, et al. Cerebral circulatory and metabolic responses to intravenously administered lorazepam. *Anesthesiology.* 1980;53:215–218.
34. Blacklock JB, Oldfield EH, Di-Chiro G, et al. Effect of barbiturate coma on glucose utilization in normal brain versus gliomas. Positron emission tomography studies. *J Neurosurg.* 1987;67:71–75.
35. Gilman S, Markel DS, Koeppe RA, et al. Cerebellar and brainstem hypometabolism in olivopontocerebellar atrophy detected with positron emission tomography. *Ann Neurol.* 1988;23:223–230.